LARGE TIME STEP HLL AND HLLC SCHEMES [*]

Marin Prebeg[1], Tore Flåtten[2] and Bernhard Müller[1]

Abstract. We present Large Time Step (LTS) extensions of the Harten-Lax-van Leer (HLL) and Harten-Lax-van Leer-Contact (HLLC) schemes. Herein, LTS denotes a class of explicit methods stable for Courant numbers greater than one. The original LTS method [R. J. LeVeque, *SIAM J. Numer. Anal.*, 22 (1985), pp. 1051–1073] was constructed as an extension of the Godunov scheme, and successive versions have been developed in the framework of Roe's approximate Riemann solver. In this paper, we formulate the LTS extension of the HLL and HLLC schemes in conservation form. We provide explicit expressions for the flux-difference splitting coefficients and the numerical viscosity coefficients of the LTS-HLL scheme. We apply the new schemes to the one-dimensional Euler equations and compare them to their non-LTS counterparts. As test cases, we consider the classical Sod shock tube problem and the Woodward-Colella blast-wave problem. We numerically demonstrate that for the right choice of wave velocity estimates both schemes calculate entropy satisfying solutions.

1991 Mathematics Subject Classification. 65M99, 35L65, 65Y20.

The dates will be set by the publisher.

1. Introduction

We consider the hyperbolic system of conservation laws:

$$\mathbf{U}_t + \mathbf{F}(\mathbf{U})_x = 0, \tag{1.1a}$$
$$\mathbf{U}(x,0) = \mathbf{U}_0(x), \tag{1.1b}$$

where $\mathbf{U} \in \mathbb{R}^N$ is the vector of conserved variables, $\mathbf{F}(\mathbf{U})$ is the flux function and $\mathbf{U}_0$ is the initial data. We are interested in solving (1.1) with an explicit finite volume method not limited by the CFL (Courant-Friedrichs-Lewy) condition.

A class of such methods has been proposed by LeVeque in a series of papers [13, 14, 15] in the 1980s. Therein, the Godunov scheme was extended to the LTS-Godunov scheme and applied to the Euler equations. The CFL condition is relaxed by allowing the waves from each Riemann problem to travel more than one cell during a single time step. Each wave is treated as a discontinuity, and the interactions between the waves are assumed to be linear. Through the years this idea has been used by a number of authors. For the shallow water equations, Murillo, Morales-Hernández and co-workers [27, 23, 25, 24, 26] applied the LTS-Roe scheme

[1] Department of Energy and Process Engineering, Norwegian University of Science and Technology, Kolbjørn Hejes vei 2, NO-7491 Trondheim, Norway; e-mail: `marin.prebeg@ntnu.no, marin.prebeg@gmail.com & bernhard.muller@ntnu.no`

[2] SINTEF Materials and Chemistry, P. O. Box 4760 Sluppen, NO-7465 Trondheim, Norway; e-mail: `toref@math.uio.no`

and Xu et al. [41] applied the LTS-Godunov scheme. Further applications of the LTS-Godunov scheme include the 3D Euler equations by Qian and Lee [31], high speed combustion waves by Tang et al. [35], and Maxwell's equations by Makwana and Chatterjee [21]. Lindqvist and Lund [18] and Prebeg et al. [30] applied the LTS-Roe scheme to two-phase flow models. Lindqvist et al. [19] also studied the TVD properties of LTS methods and showed that the LTS-Roe scheme and the LTS-Lax-Friedrichs scheme are the least and most diffusive TVD LTS methods, respectively. All the methods discussed above share the feature of starting from a Godunov or Roe-type Riemann solver and extending it to the LTS framework. The goal of this paper is to establish a more general platform for LTS extensions of approximate Riemann solvers. In particular, we will construct the natural LTS extensions of the HLL and HLLC schemes, and quantify their level of numerical diffusion.

The original HLL scheme, proposed by Harten, Lax and van Leer [9] in the 1980s, assumes a two-wave structure of the solution and constructs the approximate Riemann solver by using estimates of the velocities of the slowest and the fastest waves. The choice for these velocity estimates has been studied for instance by Davis [4], Einfeldt and co-workers [5, 6] and Batten et al. [1]. The original HLL solver may poorly resolve certain physics in systems where the solution structure consists of more than two waves. For the Euler equations, Toro et al. [39] proposed the HLLC solver in which the contact discontinuity is reconstructed by assuming a three-wave structure of the solution. Today, HLL and HLLC solvers are widely used in a number of different fields, such as multiphase flow modeling [42, 37, 36, 28, 3, 2, 20] and magnetohydrodynamics [12, 22].

In this paper, we show how LeVeque's approach [15] may be directly used to derive LTS extensions of the HLL and HLLC schemes, denoted as LTS-HLL and LTS-HLLC, respectively. In section 2 we present our basic model and numerical framework. In section 3 we present the standard HLL scheme and extend it to the LTS framework. In particular, we write the scheme in numerical viscosity and flux-difference splitting form. Section 4 presents the LTS extension of the HLLC scheme. In section 5, we study in more detail the numerical diffusion of the LTS-HLL scheme. We provide a direct proof that the numerical viscosity coefficients satisfy the TVD property without any restriction on the time step. We also prove that for subsonic flows, the numerical diffusion for the contact wave increases monotonically with the time step. This is in contrast with previously investigated LTS methods [15, 23, 19], where the numerical diffusion will typically attain local minima for integer Courant numbers. In section 6 we present numerical investigations for the one-dimensional Euler equations. The resulting LTS-HLL(C) schemes are seen to improve the efficiency of standard HLL(C) schemes while also providing improved robustness compared to previously studied LTS methods. In section 7 we close with conclusions.

2. Preliminaries

2.1. Problem outline

As a special example of (1.1) we consider the Euler equations where the vector of conserved variables $\mathbf{U}$ and the flux function $\mathbf{F}(\mathbf{U})$ are defined as:

$$\mathbf{U} = \begin{pmatrix} \rho \\ \rho u \\ E \end{pmatrix}, \qquad \mathbf{F}(\mathbf{U}) = \begin{pmatrix} \rho u \\ \rho u^2 + p \\ u(E+p) \end{pmatrix}, \tag{2.1}$$

where ρ, u, E, p denote the density, velocity, total energy density and pressure, respectively. The system is closed by the relation for the total energy density, $E = \rho e + \rho u^2 / 2$, and an equation of state for perfect gas, $e = p/(\rho(\gamma - 1))$. Throughout the paper we will use $\gamma = 1.4$ for air. Alternatively, we can write (1.1) in a quasilinear form as:

$$\mathbf{U}_t + \mathbf{A}(\mathbf{U})\mathbf{U}_x = 0, \qquad \mathbf{A}(\mathbf{U}) = \partial \mathbf{F}(\mathbf{U})/\partial \mathbf{U}. \tag{2.2}$$

We assume that the system of equations (2.2) is hyperbolic, i.e. the Jacobian matrix $\mathbf{A}$ has real eigenvalues and linearly independent eigenvectors. The eigenvalues of the Euler system (2.1) are:

$$\lambda_1 = u - a, \quad \lambda_2 = u, \quad \lambda_3 = u + a, \tag{2.3}$$

where a is the speed of sound.

2.2. Numerical methods

We discretize (1.1) by the explicit Euler method in time and the finite volume method in space:

$$\mathbf{U}_j^{n+1} = \mathbf{U}_j^n - \frac{\Delta t}{\Delta x} \left(\mathbf{F}_{j+1/2}^n - \mathbf{F}_{j-1/2}^n \right), \tag{2.4}$$

where $\mathbf{U}_j^n$ is a piecewise constant approximation of $\mathbf{U}$ in the cell with center at x_j at time level n and $\mathbf{F}_{j+1/2}^n$ is a numerical approximation of the flux function at the cell interface $x_{j+1/2}$ at time level n.

2.2.1. *Standard 3-point methods*

In the case that the numerical flux depends only on the neighboring cell values, we can with no loss of generality write the scheme in the numerical viscosity form [7, 34]:

$$\mathbf{F}_{j+1/2}^n = \mathbf{F}\left(\mathbf{U}_j^n, \mathbf{U}_{j+1}^n\right) = \frac{1}{2}\left(\mathbf{F}_j^n + \mathbf{F}_{j+1}^n\right) - \frac{1}{2}\mathbf{Q}_{j+1/2}^n\left(\mathbf{U}_{j+1}^n - \mathbf{U}_j^n\right), \tag{2.5}$$

where $\mathbf{F}_j^n = \mathbf{F}\left(\mathbf{U}_j^n\right)$ and $\mathbf{Q}_{j+1/2}^n$ is the numerical viscosity matrix. To simplify the notation, the time level n will be implicitly assumed in the absence of a temporal index. The choice of the numerical viscosity matrix $\mathbf{Q}$ determines the finite volume method we use, i.e. for the Lax-Friedrichs scheme $\mathbf{Q}_{\mathrm{LxF}} = \mathrm{diag}(\Delta x/\Delta t)$, and for the Roe scheme $\mathbf{Q}_{\mathrm{Roe}} = |\hat{\mathbf{A}}|$ where $\hat{\mathbf{A}}$ is the Roe matrix [32]. $\hat{\mathbf{A}}$ can be diagonalized as:

$$\hat{\mathbf{A}} = \hat{\mathbf{R}}\hat{\mathbf{\Lambda}}\hat{\mathbf{R}}^{-1}, \tag{2.6}$$

where $\hat{\mathbf{R}}$ is the matrix of right eigenvectors and $\hat{\mathbf{\Lambda}} = \mathrm{diag}(\lambda_1, \ldots, \lambda_N)$ is the matrix of eigenvalues. We note that in the Lax-Friedrichs and the Roe schemes, the numerical viscosity matrix $\mathbf{Q}$ acts independently on each characteristic field. In that case, $\mathbf{Q}$ can be diagonalized as:

$$\mathbf{Q} = \hat{\mathbf{R}}\mathbf{\Omega}\hat{\mathbf{R}}^{-1}, \tag{2.7}$$

where $\mathbf{\Omega} = \mathrm{diag}(\omega_1, \ldots, \omega_N)$ is the matrix of eigenvalues of $\mathbf{Q}$, and $\mathbf{Q}$ and $\hat{\mathbf{A}}$ have the same eigenvectors. The numerical viscosity matrices of the Lax-Friedrichs and the Roe scheme are then obtained by:

$$\mathbf{\Omega}_{\mathrm{LxF}} = \frac{\Delta x}{\Delta t}\mathbf{I}, \quad \mathbf{\Omega}_{\mathrm{Roe}} = |\hat{\mathbf{\Lambda}}|. \tag{2.8}$$

An alternative way to discretize (1.1) is with the flux-difference splitting:

$$\mathbf{U}_j^{n+1} = \mathbf{U}_j^n - \frac{\Delta t}{\Delta x}\left(\hat{\mathbf{A}}_{j-1/2}^+\left(\mathbf{U}_j^n - \mathbf{U}_{j-1}^n\right) + \hat{\mathbf{A}}_{j+1/2}^-\left(\mathbf{U}_{j+1}^n - \mathbf{U}_j^n\right)\right), \tag{2.9}$$

where $\hat{\mathbf{A}}^{\pm}$ represent a splitting of the Roe matrix (2.6) according to:

$$\hat{\mathbf{A}}^{\pm} = \hat{\mathbf{R}}\hat{\mathbf{\Lambda}}^{\pm}\hat{\mathbf{R}}^{-1}. \tag{2.10}$$

Herein, $\hat{\mathbf{\Lambda}}^{\pm}$ are obtained by transforming each diagonal entry of $\hat{\mathbf{\Lambda}}$:

$$\lambda_{\mathrm{LxF}}^{\pm} = \frac{1}{2}\left(\lambda \pm \frac{\Delta x}{\Delta t}\right), \quad \lambda_{\mathrm{Roe}}^{\pm} = \pm\max(0, \pm\lambda). \tag{2.11}$$

For 3-point methods, the size of the time step in discretizations (2.5) and (2.9) is limited by the CFL condition:

$$C = \max_{p,x} |\lambda_p(x,t)| \frac{\Delta t}{\Delta x} \leq 1, \tag{2.12}$$

where λ_p are the eigenvalues of the Jacobian matrix $\mathbf{A}$ in (2.2). In this paper, we consider explicit methods that are not limited by the constraint (2.12).

2.2.2. *Large Time Step methods*

The natural LTS extension of the numerical viscosity formulation (2.5) is (see [19]):

$$\mathbf{F}_{j+1/2} = \frac{1}{2} \left(\mathbf{F}_j + \mathbf{F}_{j+1} \right) - \frac{1}{2} \sum_{i=-\infty}^{\infty} \mathbf{Q}^i_{j+1/2+i} \Delta \mathbf{U}_{j+1/2+i}, \tag{2.13}$$

and the natural LTS extension of the flux-difference splitting formulation (2.9) is (see [19]):

$$\mathbf{U}_j^{n+1} = \mathbf{U}_j - \frac{\Delta t}{\Delta x} \sum_{i=0}^{\infty} \left(\hat{\mathbf{A}}^{i+}_{j-1/2-i} \Delta \mathbf{U}_{j-1/2-i} + \hat{\mathbf{A}}^{i-}_{j+1/2+i} \Delta \mathbf{U}_{j+1/2+i} \right), \tag{2.14}$$

where we introduced the notation $\Delta \mathbf{U}_{j+1/2} = \mathbf{U}_{j+1} - \mathbf{U}_j$. We note that (2.13) differs from [19] in a sense that we scale $\mathbf{Q}^i$ with $\Delta x / \Delta t$. Herein, the upper indices denote the relative cell interface position. These will be further clarified in section 3.2. Lindqvist et al. [19] provided the partial viscosity coefficients $\mathbf{Q}^i$ and the flux-difference splitting coefficients $\hat{\mathbf{A}}^{i\pm}$ for the LTS-Godunov, LTS-Roe and LTS-Lax-Friedrichs schemes. For the LTS-Roe scheme [19], the partial viscosity coefficients are defined through the eigenvalues of $\mathbf{Q}^i$:

$$\mathbf{Q}^i_{j+1/2} = \left(\hat{\mathbf{R}} \mathbf{\Omega}^i \hat{\mathbf{R}}^{-1} \right)_{j+1/2}, \tag{2.15}$$

where the eigenvalues are defined as:

$$\omega^0_{\mathrm{Roe}} = |\lambda|, \tag{2.16a}$$

$$\omega^{\mp i}_{\mathrm{Roe}} = 2 \max \left(0, \pm\lambda - i\frac{\Delta x}{\Delta t} \right), \quad \text{for } i > 0, \tag{2.16b}$$

and the flux-difference splitting coefficients are defined through the eigenvalues of $\hat{\mathbf{A}}^{i\pm}$:

$$\hat{\mathbf{A}}^{i\pm}_{j+1/2} = \left(\hat{\mathbf{R}} \hat{\mathbf{\Lambda}}^{i\pm} \hat{\mathbf{R}}^{-1} \right)_{j+1/2}, \tag{2.17}$$

where the eigenvalues are defined as:

$$\lambda^{i\pm}_{\mathrm{Roe}} = \pm \max \left(0, \min \left(\pm\lambda - i\frac{\Delta x}{\Delta t}, \frac{\Delta x}{\Delta t} \right) \right). \tag{2.18}$$

In the following section we determine these coefficients for the LTS-HLL scheme.

3. LTS-HLL SCHEME

We start by presenting the standard HLL scheme of Harten et al. [9]. Then we formulate the natural LTS extension of the HLL scheme and provide explicit expressions for the flux-difference splitting and the numerical viscosity coefficients.

3.1. **The standard HLL scheme**

We consider the cell interface Riemann problem:

$$\mathbf{U}(x,0) = \begin{cases} \mathbf{U}_j & \text{if} \quad x < 0, \\ \mathbf{U}_{j+1} & \text{if} \quad x > 0. \end{cases} \tag{3.1}$$

The original HLL scheme by Harten et al. [9] solves the Riemann problem approximately by assuming a single state between the left and right states:

$$\widetilde{\mathbf{U}}(x/t) = \begin{cases} \mathbf{U}_j & \text{if} \quad x < S_\text{L}t, \\ \mathbf{U}^{\text{HLL}}_{j+1/2} & \text{if} \quad S_\text{L}t < x < S_\text{R}t, \\ \mathbf{U}_{j+1} & \text{if} \quad x > S_\text{R}t, \end{cases} \tag{3.2}$$

where S_L and S_R are approximations of the smallest and the largest wave velocities at the interface $x_{j+1/2}$. As for now, we leave these unspecified and return to them in section 6. The intermediate state $\mathbf{U}^{\text{HLL}}_{j+1/2}$ is defined such that the Riemann solver is consistent with the integral form of the conservation law (1.1), see [9, 5]:

$$\mathbf{U}^{\text{HLL}}_{j+1/2} = \frac{S_\text{R}\mathbf{U}_{j+1} - S_\text{L}\mathbf{U}_j + \mathbf{F}_j - \mathbf{F}_{j+1}}{S_\text{R} - S_\text{L}}. \tag{3.3}$$

Next, we use $\mathbf{U}^{\text{HLL}}_{j+1/2}$ to determine the flux function $\mathbf{F}_{j+1/2}$. This is defined as:

$$\mathbf{F}_{j+1/2} = \begin{cases} \mathbf{F}_j & \text{if} \quad 0 < S_\text{L}, \\ \mathbf{F}^{\text{HLL}}_{j+1/2} & \text{if} \quad S_\text{L} < 0 < S_\text{R}, \\ \mathbf{F}_{j+1} & \text{if} \quad 0 > S_\text{R}. \end{cases} \tag{3.4}$$

In the interesting case, $S_\text{L} < 0 < S_\text{R}$, the flux function has the form [38]:

$$\mathbf{F}^{\text{HLL}}_{j+1/2} = \mathbf{F}_j + S_\text{L}\left(\mathbf{U}^{\text{HLL}}_{j+1/2} - \mathbf{U}_j\right), \tag{3.5}$$

$$\mathbf{F}^{\text{HLL}}_{j+1/2} = \mathbf{F}_{j+1} + S_\text{R}\left(\mathbf{U}^{\text{HLL}}_{j+1/2} - \mathbf{U}_{j+1}\right). \tag{3.6}$$

These two equations are equivalent and by using (3.3) in any of them we obtain:

$$\mathbf{F}^{\text{HLL}}_{j+1/2} = \frac{S_\text{R}\mathbf{F}_j - S_\text{L}\mathbf{F}_{j+1} + S_\text{L}S_\text{R}\left(\mathbf{U}_{j+1} - \mathbf{U}_j\right)}{S_\text{R} - S_\text{L}}. \tag{3.7}$$

Further, the equations (3.4) and (3.7) can be written more compactly as:

$$\mathbf{F}_{j+1/2} = \frac{S_\text{R}^+\mathbf{F}_j - S_\text{L}^-\mathbf{F}_{j+1} + S_\text{L}^- S_\text{R}^+\left(\mathbf{U}_{j+1} - \mathbf{U}_j\right)}{S_\text{R}^+ - S_\text{L}^-}, \tag{3.8}$$

where $S_\text{L}^- = \min(S_\text{L},0)$ and $S_\text{R}^+ = \max(S_\text{R},0)$. Equation (3.8) is then used in (2.4). For more information and more detailed derivation we refer to [9, 4, 5, 1, 38]. Einfeldt [5] showed that the numerical flux (3.8) can be recovered from the numerical viscosity framework (2.5) by setting:

$$\mathbf{Q}_{\text{HLL}} = \frac{S_\text{R}^+ + S_\text{L}^-}{S_\text{R}^+ - S_\text{L}^-}\hat{\mathbf{A}} - 2\frac{S_\text{L}^- S_\text{R}^+}{S_\text{R}^+ - S_\text{L}^-}\mathbf{I}. \tag{3.9}$$

Following the framework introduced in (2.8), we define the HLL scheme through the diagonal entries of $\mathbf{\Omega}$ as:

$$\omega_{\text{HLL}} = \frac{S_{\text{R}}^+(\lambda - S_{\text{L}}^-) - S_{\text{L}}^-(S_{\text{R}}^+ - \lambda)}{S_{\text{R}}^+ - S_{\text{L}}^-} = \frac{|S_{\text{R}}|\,(\lambda - S_{\text{L}}) + |S_{\text{L}}|\,(S_{\text{R}} - \lambda)}{S_{\text{R}} - S_{\text{L}}}. \tag{3.10}$$

The HLL scheme can also be written in the flux-difference splitting framework (2.11) by modifying the diagonal entries of $\hat{\mathbf{\Lambda}}^\pm$ as:

$$\lambda_{\text{HLL}}^+ = \frac{\lambda - S_{\text{L}}^-}{S_{\text{R}}^+ - S_{\text{L}}^-}S_{\text{R}}^+ = \frac{\lambda - S_{\text{L}}}{S_{\text{R}} - S_{\text{L}}}S_{\text{R}}^+ + \frac{S_{\text{R}} - \lambda}{S_{\text{R}} - S_{\text{L}}}S_{\text{L}}^+, \tag{3.11}$$

$$\lambda_{\text{HLL}}^- = \frac{S_{\text{R}}^+ - \lambda}{S_{\text{R}}^+ - S_{\text{L}}^-}S_{\text{L}}^- = \frac{\lambda - S_{\text{L}}}{S_{\text{R}} - S_{\text{L}}}S_{\text{R}}^- + \frac{S_{\text{R}} - \lambda}{S_{\text{R}} - S_{\text{L}}}S_{\text{L}}^-. \tag{3.12}$$

3.2. The LTS-HLL scheme

We want to construct the LTS extension of the numerical flux function (3.8). Consider the Figure 1a and the Riemann problem at the interface $x_{j+1/2}$. First, we consider the wave structure when $C \leq 1$, denoted in Figure 1b as $\Delta t^{\text{non-LTS}}$. In this case, the Riemann problem at $x_{j+1/2}$ is completely defined by $\mathbf{U}_j, \mathbf{U}_{j+1}$ and velocities $S_{\text{L},j+1/2}$ and $S_{\text{R},j+1/2}$ being emitted from the interface $x_{j+1/2}$, see (3.2)–(3.8). Next, we consider the case when $C > 1$, denoted in Figure 1b as Δt^{LTS}. For this case, the wave emitted from the interface $x_{j-1/2}$ and associated with velocity $S_{\text{R},j-1/2}$ passes through the interface $x_{j+1/2}$.

This wave violates the CFL condition (2.12) since we allowed the wave to travel more than one cell during a single time step. However, we may relax the CFL condition (2.12) if we modify (3.8) by taking into account this additional contribution. We start by assuming that the interactions between the waves are linear and we note that:

- The flux function (3.8) at the interface $x_{j+1/2}$ is increased by the contribution from the *jump 2* moving to the right with the velocity $S_{\text{R},j-1/2}$.
- The contribution from the *jump 2* does not start passing through the interface $x_{j+1/2}$ immediately, i.e. it has to travel through the cell x_j before it starts to pass through the interface $x_{j+1/2}$.

Based on this, we modify (3.8) as:

$$\mathbf{F}_{j+1/2}^{\text{LTS-HLL}} = \mathbf{F}_{j+1/2}^0 + S_{\text{R},j-1/2}^{-1}\left(\mathbf{U}_{j-1/2}^{\text{HLL}} - \mathbf{U}_j\right), \tag{3.13}$$

where we denoted (3.8) as $\mathbf{F}_{j+1/2}^0$, and:

$$S_{\text{R},j-1/2}^{-1} = S_{\text{R},j-1/2} - \frac{\Delta x}{\Delta t}. \tag{3.14}$$

The purpose of this modification is to take into the account the fact that the wave has to travel one cell before it starts contributing to the flux function (3.13). In the general case, we allow for an arbitrarily large time step size Δt, therefore allowing the waves to travel several cells during a single time step. In addition, we note that each interface may emit waves where each of the local wave speeds S_{L} and S_{R} may be either negative, zero or positive. Therefore, the general formula for the flux function of the LTS-HLL scheme has the form:

$$\mathbf{F}_{j+1/2}^{\text{LTS-HLL}} = \mathbf{F}_{j+1/2}^0 + \sum_{i=1}^{\infty} \mathbf{F}_{j+1/2-i}^{-i} + \sum_{i=1}^{\infty} \mathbf{F}_{j+1/2+i}^{+i}, \tag{3.15}$$

where the additional terms under the sum signs represent the information reaching the interface $x_{j+1/2}$ from neighboring Riemann problems on the left and on the right, respectively. The newly introduced terms in (3.15)
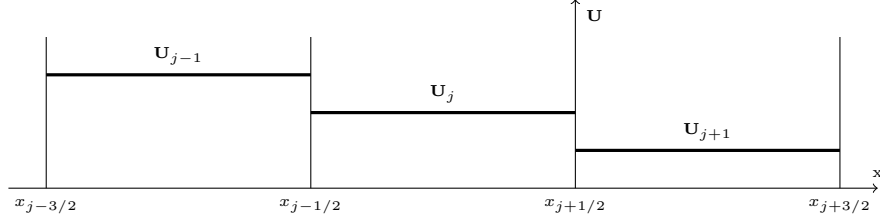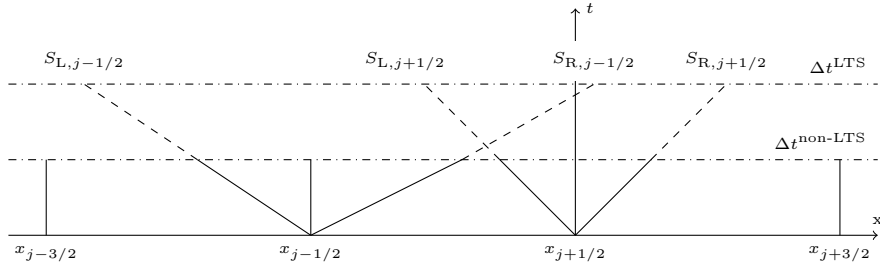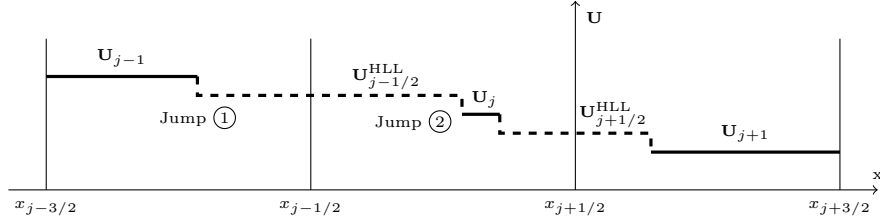
(A) Riemann problems at $x_{j-1/2}$ and $x_{j+1/2}$

(B) Characteristics with slopes $\mathrm{d}x(t)/\mathrm{d}t = S_{\mathrm{L,R}}$ at $x_{j\mp1/2}$

(C) Approximate solutions of Riemann problems at $x_{j\mp1/2}$ with HLL scheme

FIGURE 1. Wave structure in the LTS-HLL scheme

are:

$$\mathbf{F}^{-i}_{j+1/2-i} = S^{-i}_{\mathrm{R},j+1/2-i}\left(\mathbf{U}^{\mathrm{HLL}}_{j+1/2-i} - \mathbf{U}_{j+1-i}\right) + S^{-i}_{\mathrm{L},j+1/2-i}\left(\mathbf{U}_{j-i} - \mathbf{U}^{\mathrm{HLL}}_{j+1/2-i}\right), \tag{3.16}$$

$$\mathbf{F}^{+i}_{j+1/2+i} = S^{+i}_{\mathrm{L},j+1/2+i}\left(\mathbf{U}^{\mathrm{HLL}}_{j+1/2+i} - \mathbf{U}_{j+i}\right) + S^{+i}_{\mathrm{R},j+1/2+i}\left(\mathbf{U}_{j+1+i} - \mathbf{U}^{\mathrm{HLL}}_{j+1/2+i}\right), \tag{3.17}$$

where the modified wave velocities are:

$$S^{-i}_{\mathrm{[L,R]},j+1/2-i} = \max\left(S_{\mathrm{[L,R]},j+1/2-i} - i\frac{\Delta x}{\Delta t}, 0\right), \tag{3.18a}$$

$$S^{+i}_{\mathrm{[L,R]},j+1/2+i} = \min\left(S_{\mathrm{[L,R]},j+1/2+i} + i\frac{\Delta x}{\Delta t}, 0\right). \tag{3.18b}$$

Equation (3.15) is then used in (2.4).

3.2.1. The LTS-HLL scheme in numerical viscosity form

We can now write the LTS-HLL scheme in the numerical viscosity form (2.13).

Proposition 1. *Given the Roe matrix:*

$$\hat{\mathbf{A}}_{j+1/2} = \left(\hat{\mathbf{R}}\hat{\boldsymbol{\Lambda}}\hat{\mathbf{R}}^{-1}\right)_{j+1/2} \quad \forall j, \tag{3.19}$$

where $\hat{\boldsymbol{\Lambda}}$ is the diagonal matrix of eigenvalues, the LTS-HLL scheme defined by (3.13)–(3.18) can be written in the numerical viscosity form (2.13) with coefficients:

$$\mathbf{Q}^i_{j+1/2} = \left(\hat{\mathbf{R}}\boldsymbol{\Omega}^i\hat{\mathbf{R}}^{-1}\right)_{j+1/2}, \tag{3.20}$$

where $\boldsymbol{\Omega}^i(\hat{\boldsymbol{\Lambda}}, S_{\mathrm{L}}, S_{\mathrm{R}})$ is the diagonal matrix with entries given by:

$$\omega^0_{HLL} = \frac{|S_{\mathrm{R}}|\left(\lambda - S_{\mathrm{L}}\right) + |S_{\mathrm{L}}|\left(S_{\mathrm{R}} - \lambda\right)}{S_{\mathrm{R}} - S_{\mathrm{L}}}, \tag{3.21a}$$

$$\omega^{\mp i}_{HLL} = 2\frac{\lambda - S_{\mathrm{L}}}{S_{\mathrm{R}} - S_{\mathrm{L}}}\max\left(0, \pm S_{\mathrm{R}} - i\frac{\Delta x}{\Delta t}\right) + 2\frac{S_{\mathrm{R}} - \lambda}{S_{\mathrm{R}} - S_{\mathrm{L}}}\max\left(0, \pm S_{\mathrm{L}} - i\frac{\Delta x}{\Delta t}\right) \quad for \quad i > 0. \tag{3.21b}$$

Proof. The coefficient $\mathbf{Q}^0$ has already been determined by (3.9). We obtain the coefficients $\mathbf{Q}^i$ for $i \neq 0$ by equalizing (2.13) and (3.15), while using the Roe condition [32]:

$$\hat{\mathbf{A}}_{j+1/2}\left(\mathbf{U}_{j+1} - \mathbf{U}_j\right) = \mathbf{F}(\mathbf{U}_{j+1}) - \mathbf{F}(\mathbf{U}_j). \tag{3.22}$$

$\square$

We point out the similarity of the LTS-HLL partial viscosity coefficients (3.21) to the partial viscosity coefficients of the LTS-Roe scheme (2.16).

3.2.2. *The LTS-HLL scheme in flux-difference splitting form*

We have built the LTS-HLL scheme by heuristic arguments as an extension of the standard HLL scheme, following LeVeque's general approach of treating all wave interactions as linear [15]. We now derive the flux-difference splitting formulation in a more formal way, starting with LeVeque's general updating formula [15]:

$$\mathbf{U}_j^{n+1} = \frac{\Delta t}{\Delta x}\sum_{i=-\infty}^{\infty}\int_{(i-1)\frac{\Delta x}{\Delta t}}^{i\frac{\Delta x}{\Delta t}}\widetilde{\mathbf{U}}_{j+1/2-i}(\zeta_i)\,\mathrm{d}\zeta_i - \sum_{\ell=-\infty}^{\infty}\mathbf{U}_\ell, \tag{3.23}$$

where $\widetilde{\mathbf{U}}_{j+1/2-i}(\zeta_i)$ is the solution to the Riemann problem at $x_{j+1/2-i}$. Herein:

$$\zeta_i = \frac{x - x_{j+1/2-i}}{t - t^n}. \tag{3.24}$$

Proposition 2. *Given the Roe matrix:*

$$\hat{\mathbf{A}}_{j+1/2} = \left(\hat{\mathbf{R}}\hat{\boldsymbol{\Lambda}}\hat{\mathbf{R}}^{-1}\right)_{j+1/2} \quad \forall j, \tag{3.25}$$

where $\hat{\boldsymbol{\Lambda}}$ is the diagonal matrix of eigenvalues, the LTS-HLL scheme can be written in the flux-difference splitting form (2.14) with coefficients:

$$\hat{\mathbf{A}}^{i\pm}_{j+1/2} = \left(\hat{\mathbf{R}}\hat{\boldsymbol{\Lambda}}^{i\pm}\hat{\mathbf{R}}^{-1}\right)_{j+1/2}, \tag{3.26}$$

where $\hat{\mathbf{\Lambda}}^{i\pm}(\hat{\mathbf{\Lambda}}, S_{\mathrm{L}}, S_{\mathrm{R}})$ is the diagonal matrix with entries given by:

$$\lambda_{HLL}^{i\pm} = \pm \frac{\lambda - S_{\mathrm{L}}}{S_{\mathrm{R}} - S_{\mathrm{L}}} \max\left(0, \min\left(\pm S_{\mathrm{R}} - i\frac{\Delta x}{\Delta t}, \frac{\Delta x}{\Delta t}\right)\right) \pm \frac{S_{\mathrm{R}} - \lambda}{S_{\mathrm{R}} - S_{\mathrm{L}}} \max\left(0, \min\left(\pm S_{\mathrm{L}} - i\frac{\Delta x}{\Delta t}, \frac{\Delta x}{\Delta t}\right)\right). \quad (3.27)$$

Proof. The HLL Riemann solver (3.2) can be written as:

$$\widetilde{\mathbf{U}}_{j+1/2}(\zeta) = \mathbf{U}_j + H(\zeta - S_{\mathrm{L}})\left(\mathbf{U}_{j+1/2}^{\mathrm{HLL}} - \mathbf{U}_j\right) + H(\zeta - S_{\mathrm{R}})\left(\mathbf{U}_{j+1} - \mathbf{U}_{j+1/2}^{\mathrm{HLL}}\right) \quad (3.28a)$$

$$= \mathbf{U}_{j+1} - H(S_{\mathrm{L}} - \zeta)\left(\mathbf{U}_{j+1/2}^{\mathrm{HLL}} - \mathbf{U}_j\right) - H(S_{\mathrm{R}} - \zeta)\left(\mathbf{U}_{j+1} - \mathbf{U}_{j+1/2}^{\mathrm{HLL}}\right), \quad (3.28b)$$

where H is the Heaviside function. Using (3.3) we can rewrite this as:

$$\widetilde{\mathbf{U}}_{j+1/2}(\zeta) = \mathbf{U}_j + \left(\frac{H(\zeta - S_{\mathrm{L}})}{S_{\mathrm{R}} - S_{\mathrm{L}}}(\mathbf{S}_{\mathrm{R}} - \hat{\mathbf{A}}) + \frac{H(\zeta - S_{\mathrm{R}})}{S_{\mathrm{R}} - S_{\mathrm{L}}}(\hat{\mathbf{A}} - \mathbf{S}_{\mathrm{L}})\right)(\mathbf{U}_{j+1} - \mathbf{U}_j) \quad (3.29a)$$

$$= \mathbf{U}_{j+1} - \left(\frac{H(S_{\mathrm{L}} - \zeta)}{S_{\mathrm{R}} - S_{\mathrm{L}}}(\mathbf{S}_{\mathrm{R}} - \hat{\mathbf{A}}) + \frac{H(S_{\mathrm{R}} - \zeta)}{S_{\mathrm{R}} - S_{\mathrm{L}}}(\hat{\mathbf{A}} - \mathbf{S}_{\mathrm{L}})\right)(\mathbf{U}_{j+1} - \mathbf{U}_j), \quad (3.29b)$$

where $\mathbf{S}_{\mathrm{L}} = S_{\mathrm{L}}\mathbf{I}$ and $\mathbf{S}_{\mathrm{R}} = S_{\mathrm{R}}\mathbf{I}$. We then use (3.29a) in (3.23) and note that for $i \leq 0$ we can write:

$$\int_{(i-1)\frac{\Delta x}{\Delta t}}^{i\frac{\Delta x}{\Delta t}} \widetilde{\mathbf{U}}_{j+1/2-i}(\zeta_i)\, \mathrm{d}\zeta_i = \frac{\Delta x}{\Delta t}\mathbf{U}_{j-i} - \hat{\mathbf{A}}_{j+1/2-i}^{(-i)-}\left(\mathbf{U}_{j+1-i} - \mathbf{U}_{j-i}\right), \quad (3.30)$$

where:

$$\hat{\mathbf{A}}^{i-} = \hat{\mathbf{R}}\hat{\mathbf{\Lambda}}^{i-}\hat{\mathbf{R}}^{-1}, \quad (3.31)$$

and $\hat{\mathbf{\Lambda}}^{i-}$ is the diagonal matrix with values:

$$\lambda^{i-} = \frac{\lambda - S_{\mathrm{L}}}{S_{\mathrm{R}} - S_{\mathrm{L}}} \min\left(0, \max\left(S_{\mathrm{R}} + i\frac{\Delta x}{\Delta t}, -\frac{\Delta x}{\Delta t}\right)\right) + \frac{S_{\mathrm{R}} - \lambda}{S_{\mathrm{R}} - S_{\mathrm{L}}} \min\left(0, \max\left(S_{\mathrm{L}} + i\frac{\Delta x}{\Delta t}, -\frac{\Delta x}{\Delta t}\right)\right). \quad (3.32)$$

Similarly, we use (3.29b) in (3.23) and note that for $i \geq 1$ we can write:

$$\int_{(i-1)\frac{\Delta x}{\Delta t}}^{i\frac{\Delta x}{\Delta t}} \widetilde{\mathbf{U}}_{j+1/2-i}(\zeta_i)\, \mathrm{d}\zeta_i = \frac{\Delta x}{\Delta t}\mathbf{U}_{j+1-i} - \hat{\mathbf{A}}_{j+1/2-i}^{(i-1)+}\left(\mathbf{U}_{j+1-i} - \mathbf{U}_{j-i}\right), \quad (3.33)$$

where:

$$\hat{\mathbf{A}}^{i+} = \hat{\mathbf{R}}\hat{\mathbf{\Lambda}}^{i+}\hat{\mathbf{R}}^{-1}, \quad (3.34)$$

and $\hat{\mathbf{\Lambda}}^{i+}$ is the diagonal matrix with values:

$$\lambda^{i+} = \frac{\lambda - S_{\mathrm{L}}}{S_{\mathrm{R}} - S_{\mathrm{L}}} \max\left(0, \min\left(S_{\mathrm{R}} - i\frac{\Delta x}{\Delta t}, \frac{\Delta x}{\Delta t}\right)\right) + \frac{S_{\mathrm{R}} - \lambda}{S_{\mathrm{R}} - S_{\mathrm{L}}} \max\left(0, \min\left(S_{\mathrm{L}} - i\frac{\Delta x}{\Delta t}, \frac{\Delta x}{\Delta t}\right)\right). \quad (3.35)$$

Substituting (3.30) and (3.33) into (3.23) we recover the LTS flux-difference splitting equation (2.14). $\square$

We point out the similarity of the LTS-HLL flux-difference splitting coefficients (3.27) to the flux-difference splitting coefficients of the LTS-Roe scheme (2.18).

Proposition 3. *The flux-difference splitting formulation* (3.26)–(3.27) *and the numerical viscosity formulation* (3.20)–(3.21) *are equivalent.*

Proof. Lindqvist et al. [19] derived the following one-to-one mapping between the numerical viscosity and flux-difference splitting coefficients:

$$\mathbf{A}^{0\pm} = \frac{1}{2} \left(\mathbf{A} \pm \mathbf{Q}^0 \mp \mathbf{Q}^{\mp 1} \right), \quad \mathbf{A}^{i\pm} = \pm \frac{1}{2} \left(\mathbf{Q}^{\mp i} - \mathbf{Q}^{\mp(i+1)} \right). \tag{3.36}$$

By using (3.20)–(3.21) in (3.36) we obtain (3.26)–(3.27). □

4. LTS-HLLC scheme

In this section we propose a direct extension from the HLLC scheme to the LTS-HLLC scheme, following the approaches from section 3.

4.1. Standard HLLC scheme

We recall that the standard HLL scheme assumes a two wave structure of the solution with a single, uniform state $\mathbf{U}^{\mathrm{HLL}}$ between the waves. This is a correct assumption for hyperbolic systems consisting of only two equations (such as the one-dimensional shallow water equations). However, for the Euler equations this assumption leads to neglecting the contact discontinuity. The approach to recover the missing contact discontinuity was first presented by Toro et al. [39]. Herein, we outline an approach to reconstruct the missing wave following the approach described by Toro in [38].

The standard HLLC scheme is given in the form similar to the HLL scheme defined by equations (3.2) and (3.4), but with the state $\mathbf{U}^{\mathrm{HLL}}$ being split into two states separated by a contact discontinuity:

$$\widetilde{\mathbf{U}}(x/t) = \begin{cases} \mathbf{U}_j & \text{if} \quad x < S_{\mathrm{L}} t, \\ \mathbf{U}_{\mathrm{L}}^{\mathrm{HLLC}} & \text{if} \quad S_{\mathrm{L}} t < x < S_{\mathrm{C}} t, \\ \mathbf{U}_{\mathrm{R}}^{\mathrm{HLLC}} & \text{if} \quad S_{\mathrm{C}} t < x < S_{\mathrm{R}} t, \\ \mathbf{U}_{j+1} & \text{if} \quad x > S_{\mathrm{R}} t. \end{cases} \tag{4.1}$$

Based on this, the numerical flux function is defined as:

$$\mathbf{F}_{j+1/2} = \begin{cases} \mathbf{F}_j & \text{if} \quad 0 < S_{\mathrm{L}}, \\ \mathbf{F}_{\mathrm{L},j+1/2}^{\mathrm{HLLC}} & \text{if} \quad S_{\mathrm{L}} < 0 < S_{\mathrm{C}}, \\ \mathbf{F}_{\mathrm{R},j+1/2}^{\mathrm{HLLC}} & \text{if} \quad S_{\mathrm{C}} < 0 < S_{\mathrm{R}}, \\ \mathbf{F}_{j+1} & \text{if} \quad 0 > S_{\mathrm{R}}. \end{cases} \tag{4.2}$$

In the interesting case, $S_{\mathrm{L}} < 0 < S_{\mathrm{R}}$, the numerical flux function has the form:

$$\mathbf{F}_{\mathrm{L},j+1/2}^{\mathrm{HLLC}} = \mathbf{F}_j + S_{\mathrm{L}} \left(\mathbf{U}_{\mathrm{L},j+1/2}^{\mathrm{HLLC}} - \mathbf{U}_j \right), \tag{4.3}$$

$$\mathbf{F}_{\mathrm{R},j+1/2}^{\mathrm{HLLC}} = \mathbf{F}_{j+1} + S_{\mathrm{R}} \left(\mathbf{U}_{\mathrm{R},j+1/2}^{\mathrm{HLLC}} - \mathbf{U}_{j+1} \right), \tag{4.4}$$

where the intermediate states are determined according to [38]:

$$\mathbf{U}_{\mathrm{K}}^{\mathrm{HLLC}} = \rho_{\mathrm{K}} \left(\frac{S_{\mathrm{K}} - u_{\mathrm{K}}}{S_{\mathrm{K}} - S_{\mathrm{C}}} \right) \begin{bmatrix} 1 \\ S_{\mathrm{C}} \\ \frac{E_{\mathrm{K}}}{\rho_{\mathrm{K}}} + (S_{\mathrm{C}} - u_{\mathrm{K}}) \left(S_{\mathrm{C}} + \frac{p_{\mathrm{K}}}{\rho_{\mathrm{K}}(S_{\mathrm{K}} - u_{\mathrm{K}})} \right) \end{bmatrix}, \tag{4.5}$$

where index K denotes left (L) or right (R) state in (4.1). The contact discontinuity velocity is given by [38]:

$$S_{\mathrm{C}} = \frac{p_{\mathrm{R}} - p_{\mathrm{L}} + \rho_{\mathrm{L}} u_{\mathrm{L}}(S_{\mathrm{L}} - u_{\mathrm{L}}) - \rho_{\mathrm{R}} u_{\mathrm{R}}(S_{\mathrm{R}} - u_{\mathrm{R}})}{\rho_{\mathrm{L}}(S_{\mathrm{L}} - u_{\mathrm{L}}) - \rho_{\mathrm{R}}(S_{\mathrm{R}} - u_{\mathrm{R}})}. \tag{4.6}$$

For details on the derivation of these formulae we refer to the book by Toro [38].

4.2. LTS-HLLC scheme

Following the approaches of section 3, we obtain the following expression for the numerical flux to be used in (2.4):

Proposition 4. *The numerical flux of the LTS-HLLC scheme (4.2) is:*

$$\mathbf{F}_{j+1/2}^{LTS\text{-}HLLC} = \mathbf{F}_{j+1/2}^0 + \sum_{i=1}^{\infty} \mathbf{F}_{j+1/2-i}^{-i} + \sum_{i=1}^{\infty} \mathbf{F}_{j+1/2+i}^{+i}, \tag{4.7}$$

where $\mathbf{F}_{j+1/2}^0$ *is the standard HLLC flux given by (4.2), and the additional terms are:*

$$\begin{aligned}
\mathbf{F}_{j+1/2-i}^{-i} &= S_{R,j+1/2-i}^{-i}\left(\mathbf{U}_{R,j+1/2-i}^{HLLC} - \mathbf{U}_{j+1-i}\right) \\
&\quad + S_{C,j+1/2-i}^{-i}\left(\mathbf{U}_{L,j+1/2-i}^{HLLC} - \mathbf{U}_{R,j+1/2-i}^{HLLC}\right) \\
&\quad + S_{L,j+1/2-i}^{-i}\left(\mathbf{U}_{j-i} - \mathbf{U}_{L,j+1/2-i}^{HLLC}\right),
\end{aligned} \tag{4.8}$$

$$\begin{aligned}
\mathbf{F}_{j+1/2+i}^{+i} &= S_{L,j+1/2+i}^{+i}\left(\mathbf{U}_{L,j+1/2+i}^{HLLC} - \mathbf{U}_{j+i}\right) \\
&\quad + S_{C,j+1/2+i}^{+i}\left(\mathbf{U}_{R,j+1/2+i}^{HLLC} - \mathbf{U}_{L,j+1/2+i}^{HLLC}\right) \\
&\quad + S_{R,j+1/2+i}^{+i}\left(\mathbf{U}_{j+1+i} - \mathbf{U}_{R,j+1/2+i}^{HLLC}\right).
\end{aligned} \tag{4.9}$$

Herein, the modified velocities are:

$$S_{[L,C,R],j+1/2-i}^{-i} = \max\left(S_{[L,C,R],j+1/2-i} - i\frac{\Delta x}{\Delta t}, 0\right), \tag{4.10}$$

$$S_{[L,C,R],j+1/2+i}^{+i} = \min\left(S_{[L,C,R],j+1/2+i} + i\frac{\Delta x}{\Delta t}, 0\right). \tag{4.11}$$

Proof. The HLLC Riemann solver (4.1) can be written as:

$$\begin{aligned}
\widetilde{\mathbf{U}}_{j+1/2}(\zeta) &= \mathbf{U}_j + H(\zeta - S_{\mathrm{L}})\left(\mathbf{U}_{\mathrm{L}}^{\mathrm{HLLC}} - \mathbf{U}_j\right) \\
&\quad + H(\zeta - S_{\mathrm{C}})\left(\mathbf{U}_{\mathrm{R}}^{\mathrm{HLLC}} - \mathbf{U}_{\mathrm{L}}^{\mathrm{HLLC}}\right) + H(\zeta - S_{\mathrm{R}})\left(\mathbf{U}_{j+1} - \mathbf{U}_{\mathrm{R}}^{\mathrm{HLLC}}\right),
\end{aligned} \tag{4.12}$$

or equivalently:

$$\begin{aligned}
\widetilde{\mathbf{U}}_{j+1/2}(\zeta) &= \mathbf{U}_{j+1} - H(S_{\mathrm{L}} - \zeta)\left(\mathbf{U}_{\mathrm{L}}^{\mathrm{HLLC}} - \mathbf{U}_j\right) \\
&\quad - H(S_{\mathrm{C}} - \zeta)\left(\mathbf{U}_{\mathrm{R}}^{\mathrm{HLLC}} - \mathbf{U}_{\mathrm{L}}^{\mathrm{HLLC}}\right) - H(S_{\mathrm{R}} - \zeta)\left(\mathbf{U}_{j+1} - \mathbf{U}_{\mathrm{R}}^{\mathrm{HLLC}}\right),
\end{aligned} \tag{4.13}$$

where H is the Heaviside function and ζ is given by (3.24). We then use (4.12) in (3.23) and note that for $i \leq 0$ we can write:

$$
\int_{(i-1)\frac{\Delta x}{\Delta t}}^{i\frac{\Delta x}{\Delta t}} \widetilde{\mathbf{U}}_{j+1/2-i}(\zeta_i)\,\mathrm{d}\zeta_i = \frac{\Delta x}{\Delta t}\mathbf{U}_{j-i}
$$

$$
+ \left(\min\left(0, S_\mathrm{L} - (i-1)\frac{\Delta x}{\Delta t}\right) - \min\left(0, S_\mathrm{L} - i\frac{\Delta x}{\Delta t}\right) \right) (\mathbf{U}_\mathrm{L}^\mathrm{HLLC} - \mathbf{U}_{j-i})
$$

$$
+ \left(\min\left(0, S_\mathrm{C} - (i-1)\frac{\Delta x}{\Delta t}\right) - \min\left(0, S_\mathrm{C} - i\frac{\Delta x}{\Delta t}\right) \right) (\mathbf{U}_\mathrm{R}^\mathrm{HLLC} - \mathbf{U}_\mathrm{L}^\mathrm{HLLC})
$$

$$
+ \left(\min\left(0, S_\mathrm{R} - (i-1)\frac{\Delta x}{\Delta t}\right) - \min\left(0, S_\mathrm{R} - i\frac{\Delta x}{\Delta t}\right) \right) (\mathbf{U}_{j+1-i} - \mathbf{U}_\mathrm{R}^\mathrm{HLLC}). \quad (4.14)
$$

Similarly, we use (4.13) in (3.23) and note that for $i \geq 1$ we can write:

$$
\int_{(i-1)\frac{\Delta x}{\Delta t}}^{i\frac{\Delta x}{\Delta t}} \widetilde{\mathbf{U}}_{j+1/2-i}(\zeta_i)\,\mathrm{d}\zeta_i = \frac{\Delta x}{\Delta t}\mathbf{U}_{j+1-i}
$$

$$
+ \left(\max\left(0, S_\mathrm{L} - (i-1)\frac{\Delta x}{\Delta t}\right) - \max\left(0, S_\mathrm{L} - i\frac{\Delta x}{\Delta t}\right) \right) (\mathbf{U}_\mathrm{L}^\mathrm{HLLC} - \mathbf{U}_{j-i})
$$

$$
+ \left(\max\left(0, S_\mathrm{C} - (i-1)\frac{\Delta x}{\Delta t}\right) - \max\left(0, S_\mathrm{C} - i\frac{\Delta x}{\Delta t}\right) \right) (\mathbf{U}_\mathrm{R}^\mathrm{HLLC} - \mathbf{U}_\mathrm{L}^\mathrm{HLLC})
$$

$$
+ \left(\max\left(0, S_\mathrm{R} - (i-1)\frac{\Delta x}{\Delta t}\right) - \max\left(0, S_\mathrm{R} - i\frac{\Delta x}{\Delta t}\right) \right) (\mathbf{U}_{j+1-i} - \mathbf{U}_\mathrm{R}^\mathrm{HLLC}). \quad (4.15)
$$

Herein, the index $_{j+1/2-i}$ is implicitly assumed on the parameters $S_{[\mathrm{L,C,R}]}$ and $\mathbf{U}_{[\mathrm{L,R}]}^\mathrm{HLLC}$. Using (4.14) and (4.15) in (3.23) we can write the LTS-HLLC scheme as:

$$
\mathbf{U}_j^{n+1} = \mathbf{U}_j^n - \frac{\Delta t}{\Delta x}\left(\mathbf{F}_{j+1/2}^\mathrm{LTS\text{-}HLLC} - \mathbf{F}_{j-1/2}^\mathrm{LTS\text{-}HLLC}\right). \quad (4.16)
$$

$\square$

We note that (4.8) and (4.9) are very similar to the corresponding numerical flux functions for the LTS-HLL scheme, (3.16) and (3.17), but with the addition of the middle wave associated with S_C.

5. TVD analysis and modified equation

We interpret the LTS-HLL scheme as a numerical method for the scalar conservation law and we show that the LTS-HLL scheme is TVD. Next, we employ the modified equation analysis and use the results of Lindqvist et al. [19] and Prebeg [29] to study the numerical diffusion of the LTS-HLL scheme.

5.1. **TVD analysis**

The original HLL scheme [9] and the HLLC scheme [39] have been constructed as approximate Riemann solvers for hyperbolic systems of conservation laws. However, we may interpret the standard HLL and the LTS-HLL scheme as a numerical method for scalar conservation laws with two input parameters S_L and S_R. This allows us to perform the TVD analysis of the scheme.

For the standard HLL scheme Einfeldt [5] showed that the HLL scheme satisfies the TVD-type condition if the eigenvalues ω_HLL of the numerical viscosity matrix $\mathbf{Q}_\mathrm{HLL}$ satisfy:

$$
|\lambda_{p,\mathrm{Roe}}| \leq \omega_{p,\mathrm{HLL}}, \quad (5.1)
$$

for each characteristic field p. The set of TVD conditions for LTS methods for scalar conservation laws was determined by Jameson and Lax [10, 11] (see also Lindqvist et al. [19]).

Lemma 1. *A multipoint conservative scheme in the form* (2.13) *is unconditionally TVD if and only if:*

$$2\left(\Delta x/\Delta t\right) - 2Q_{j+1/2}^0 + Q_{j+1/2}^{-1} + Q_{j+1/2}^1 \geq 0, \tag{5.2a}$$

$$Q_{j+1/2}^0 - 2Q_{j+1/2}^{\pm 1} + Q_{j+1/2}^{\pm 2} \mp \lambda_{j+1/2} \geq 0, \tag{5.2b}$$

$$Q_{j+1/2}^{\pm i} - 2Q_{j+1/2}^{\pm(i+1)} + Q_{j+1/2}^{\pm(i+2)} \geq 0, \quad \forall \quad i \geq 1, \tag{5.2c}$$

for all j, where Q are the numerical viscosity coefficients.

By interpreting the numerical viscosity coefficients of the LTS-HLL scheme (3.21) as the numerical viscosity coefficients Q of the numerical method for the scalar conservation law we may show that:

Proposition 5. *The LTS-HLL scheme is TVD under the condition:*

$$S_{\mathrm{L}} \leq \lambda \leq S_{\mathrm{R}}. \tag{5.3}$$

Proof. By substituting (3.21) in (5.2a)–(5.2c) the TVD conditions become:

$$(\lambda - S_{\mathrm{L}}) \left(\frac{\Delta x}{\Delta t} - \min\left(|S_{\mathrm{R}}|, \frac{\Delta x}{\Delta t} \right) \right)$$
$$+ (S_{\mathrm{R}} - \lambda) \left(\frac{\Delta x}{\Delta t} - \min\left(|S_{\mathrm{L}}|, \frac{\Delta x}{\Delta t} \right) \right) \geq 0, \tag{5.4a}$$

$$(\lambda - S_{\mathrm{L}}) \max\left(0, \min\left(\pm 2 S_{\mathrm{R}}, 4\frac{\Delta x}{\Delta t} \mp 2 S_{\mathrm{R}} \right) \right)$$
$$+ (S_{\mathrm{R}} - \lambda) \max\left(0, \min\left(\pm 2 S_{\mathrm{L}}, 4\frac{\Delta x}{\Delta t} \mp 2 S_{\mathrm{L}} \right) \right) \geq 0, \tag{5.4b}$$

$$(\lambda - S_{\mathrm{L}}) \max\left(0, \min\left(\pm S_{\mathrm{R}} - i\frac{\Delta x}{\Delta t}, \mp S_{\mathrm{R}} + i\frac{\Delta x}{\Delta t} + 2 \right) \right)$$
$$+ (S_{\mathrm{R}} - \lambda) \max\left(0, \min\left(\pm S_{\mathrm{L}} - i\frac{\Delta x}{\Delta t}, \mp S_{\mathrm{L}} + i\frac{\Delta x}{\Delta t} + 2 \right) \right) \geq 0, \quad \forall \quad i \geq 1, \tag{5.4c}$$

which are always satisfied under the condition (5.3). □

In the limit $\lambda = S_{\mathrm{L}} = S_{\mathrm{R}}$, we recover the LTS-Roe scheme which is well established to be TVD [15, 19].

5.2. Modified equation analysis

Once we have obtained the partial viscosity coefficients $\mathbf{Q}^i$, we may use them to compare the amount of the numerical diffusion between different schemes. One way of doing this is by employing the modified equation analysis.

Lindqvist et al. [19] showed that for the scalar conservation law the LTS scheme (2.13) and (2.14) gives a second-order accurate approximation to the equation:

$$u_t + f(u)_x = \frac{1}{2} \frac{\Delta x^2}{\Delta t} \left[\left(\sum_{i=1-k}^{k-1} \frac{\Delta t}{\Delta x} \bar{Q}^i - c^2 \right) u_x \right]_x, \tag{5.5}$$

where $\bar{Q}^i = Q^i(u, \ldots, u)$ is the numerical viscosity coefficient of the $(2k+1)$-point scheme, and $c = f'(u)\Delta t/\Delta x$. We distinguish between the numerical diffusion inherent to the scheme:

$$D(u) = \sum_{i=1-k}^{k-1} \frac{\Delta t}{\Delta x} \bar{Q}^i - c^2, \tag{5.6}$$

and the total numerical diffusion ν:

$$\nu(u) = \frac{1}{2} \frac{\Delta x^2}{\Delta t} D(u). \tag{5.7}$$

Lindqvist et al. [19] determined $D(u)$ for the LTS-Roe and LTS-Lax-Friedrichs scheme as:

$$D_{\text{LTS-Roe}} = (\lceil |c| \rceil - |c|)(1 + |c| - \lceil |c| \rceil), \tag{5.8}$$

$$D_{\text{LTS-LxF}} = k^2 - c^2, \tag{5.9}$$

where $\lceil c \rceil = \min\{n \in \mathbb{Z} \mid n \geq c\}$ is the ceiling function. By using the numerical viscosity coefficients (3.21) in (5.6), Prebeg [29] determined $D(u)$ for the LTS-HLL scheme as:

$$\begin{aligned} D_{\text{LTS-HLL}} = {} & \frac{c - c_{\text{L}}}{c_{\text{R}} - c_{\text{L}}} (\lceil |c_{\text{R}}| \rceil - |c_{\text{R}}|)(1 + |c_{\text{R}}| - \lceil |c_{\text{R}}| \rceil) \\ & + \frac{c_{\text{R}} - c}{c_{\text{R}} - c_{\text{L}}} (\lceil |c_{\text{L}}| \rceil - |c_{\text{L}}|)(1 + |c_{\text{L}}| - \lceil |c_{\text{L}}| \rceil) \\ & + (c - c_{\text{L}})(c_{\text{R}} - c), \end{aligned} \tag{5.10}$$

where $c_{\text{L}} = S_{\text{L}}\Delta t/\Delta x$ and $c_{\text{R}} = S_{\text{R}}\Delta t/\Delta x$. We use equations (5.8)–(5.10) to investigate the numerical diffusion of the LTS-Roe, LTS-Lax-Friedrichs and LTS-HLL schemes.

We consider the Euler equations and investigate the numerical diffusion at a Riemann problem with subsonic flow conditions and the Roe eigenvalues defined as:

$$\lambda_1 = -0.5, \quad \lambda_2 = 0.25, \quad \lambda_3 = 1. \tag{5.11}$$

Figure 2 shows D_p and ν_p for the p-th characteristic field as a function of the global Courant number $\bar{c}$. We use the global Courant number as an input variable and determine the time step from it as:

$$\Delta t_{\bar{c}} = \frac{\bar{c}\Delta x}{\max(|\lambda_1|, |\lambda_2|, |\lambda_3|)}. \tag{5.12}$$

Then the numerical diffusion D_p and ν_p are determined as functions of the local eigenvalue λ_p and the global time step size $\Delta t_{\bar{c}}$:

$$D_p = D(\lambda_p, \Delta t_{\bar{c}}, \Delta x), \quad \nu_p = \nu(\lambda_p, \Delta t_{\bar{c}}, \Delta x), \tag{5.13}$$

where we note that for the Figure 2 we use $S_{\text{L}} = \lambda_1$ and $S_{\text{R}} = \lambda_3$, and we assume that $\Delta x = 1$.

We observe that the area between LTS-Roe and LTS-Lax-Friedrichs curves (including the curves) is the TVD-type region. This follows from the result in [19] where it is shown that the LTS-Roe is the least diffusive and that the LTS-Lax-Friedrichs is the most diffusive TVD scheme. The range of numerical diffusion that can be achieved by the LTS-HLL scheme is hatched. Einfeldt [5] showed that for subsonic flow conditions, the standard HLL scheme can reproduce the full span of numerical diffusion between the Roe and Lax-Friedrichs schemes in the 1st and 3rd characteristic field corresponding to either shock or rarefaction. The amount of diffusion in 2nd characteristic field (contact discontinuity) is always higher than in the Roe scheme.
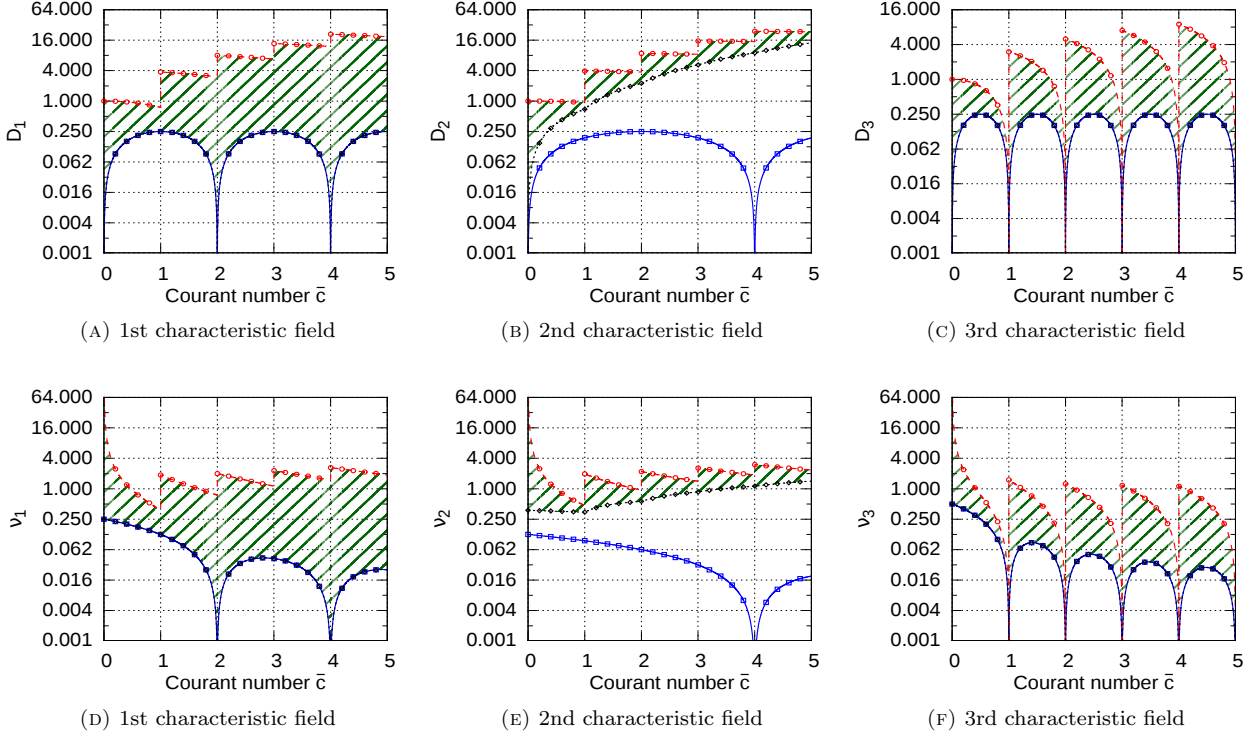
FIGURE 2. Numerical diffusion $D(u)$ and $\nu(u)$ in characteristic fields of the Euler equations for (5.11). LTS-Roe (blue-squares), LTS-Lax-Friedrichs (red-circles), LTS-HLL (black-diamonds). Hatched region (dark green-lines) is the range of numerical diffusion that can be achieved by the LTS-HLL scheme by varying S_L and S_R.

We may show that in the subsonic case, the numerical diffusion of the LTS-HLL scheme in the 2nd characteristic field is always bigger than the numerical diffusion of the LTS-Roe scheme and that it is always increasing with the time step.

Proposition 6. *The numerical diffusion of the LTS-HLL scheme in the 2nd characteristic field:*

$$D_{2,LTS\text{-}HLL} = \frac{c_2 - c_\mathrm{L}}{c_\mathrm{R} - c_\mathrm{L}} \mathcal{H}\left(|c_\mathrm{R}|\right) + \frac{c_\mathrm{R} - c_2}{c_\mathrm{R} - c_\mathrm{L}} \mathcal{H}\left(|c_\mathrm{L}|\right) + \left(c_2 - c_\mathrm{L}\right)\left(c_\mathrm{R} - c_2\right), \tag{5.14}$$

where we define:

$$c_\mathrm{L} = c_2 - \sigma, \quad c_\mathrm{R} = c_2 + \sigma, \tag{5.15}$$

with:

$$c_2 = \lambda_2 \frac{\Delta t}{\Delta x}, \quad \sigma = a \frac{\Delta t}{\Delta x}, \tag{5.16}$$

and where:

$$\mathcal{H}(|x|) = \lceil |x| \rceil + 2|x|\lceil |x| \rceil - |x| - |x|^2 - \lceil |x| \rceil^2, \tag{5.17}$$

and:

$$S_\mathrm{L} < 0 < |\lambda_2| < S_\mathrm{R}, \tag{5.18}$$

is a monotone function of the time step Δt.

Proof. By using (5.15), we can rewrite (5.14) as:

$$D_{2,\text{LTS-HLL}} = \frac{1}{2}\mathcal{H}\left(|c_\text{R}|\right) + \frac{1}{2}\mathcal{H}\left(|c_\text{L}|\right) + \sigma^2. \tag{5.19}$$

We introduce the dimensionless parameter z:

$$z = \frac{\Delta t_z}{\Delta t}, \tag{5.20}$$

and note that showing that (5.19) is a monotonically increasing function of Δt_z is equivalent to showing that:

$$D(z) = \frac{1}{2}\mathcal{H}\left(z\,|c_\text{R}|\right) + \frac{1}{2}\mathcal{H}\left(z\,|c_\text{L}|\right) + z^2\sigma^2, \tag{5.21}$$

is a monotonically increasing function of z. We note that $\mathcal{H}$ is a continuous function of x, hence $D(z)$ is also a continuous function of z. Therefore $D(z)$ is monotonically increasing if the first derivative is always positive. In other words, we need to show:

$$\frac{\mathrm{d}D(z)}{\mathrm{d}z} = |c_\text{R}|\left(\lceil z\,|c_\text{R}|\rceil - z\,|c_\text{R}|\right) + |c_\text{L}|\left(\lceil z\,|c_\text{L}|\rceil - z\,|c_\text{L}|\right) - \frac{1}{2}\left(|c_\text{L}| + |c_\text{R}|\right) + 2z\sigma^2 > 0 \quad \forall z > 0. \tag{5.22}$$

We define the maximum Courant number:

$$c_\text{max} = \max\left(|zc_\text{L}|, |zc_\text{R}|\right), \tag{5.23}$$

and consider the cases $c_\text{max} \leq 1$ and $c_\text{max} > 1$.

Case $c_\text{max} > 1$:

The first two terms in (5.22) are non-negative, so it is sufficient to show that:

$$-\frac{1}{2}\left(|c_\text{L}| + |c_\text{R}|\right) + 2z\sigma^2 > 0. \tag{5.24}$$

For subsonic flows we have that:

$$\frac{1}{2}\left(|c_\text{L}| + |c_\text{R}|\right) = \frac{1}{2}\left(c_\text{R} - c_\text{L}\right) = \sigma. \tag{5.25}$$

Hence (5.24) becomes:

$$z\sigma > \frac{1}{2}. \tag{5.26}$$

By using (5.16) we have that:

$$a\frac{\Delta t_z}{\Delta x} > \frac{1}{2}, \tag{5.27}$$

which always holds for subsonic flows when $c_\text{max} > 1$.

Case $c_\text{max} \leq 1$:

For $c_\text{max} \leq 1$ the equation (5.22) becomes:

$$\frac{\mathrm{d}D(z)}{\mathrm{d}z} = (c_2 + \sigma)(1 - zc_2 - z\sigma) - (c_2 - \sigma)(1 + zc_2 - z\sigma) - \sigma + 2z\sigma^2 > 0, \tag{5.28}$$

which simplifies to:

$$\frac{\mathrm{d}D(z)}{\mathrm{d}z} = \sigma - 2\left(c_2\right)^2 z > 0. \tag{5.29}$$

We have already proved that the expression is positive for $z > 1/(2\sigma)$, in the opposite case the lowest value of (5.29) is attained for:

$$z = \frac{1}{2\sigma},\tag{5.30}$$

giving:

$$\frac{\mathrm{d}D(z)}{\mathrm{d}z} = \sigma - \frac{(c_2)^2}{\sigma} = \frac{1}{\sigma}\left(\sigma - c_2\right)\left(\sigma + c_2\right),\tag{5.31}$$

which is always positive for subsonic flows. □

6. Results

In this section we compare the new schemes with their non-LTS counterparts and the LTS-Roe scheme. Until now, we did not discuss how to choose the wave velocity estimates for S_L and S_R in the HLL and HLLC schemes and their LTS extensions. For our investigations, the choice of wave velocity estimates for S_L and S_R is made according to Einfeldt [5]:

$$S_{\mathrm{L},j+1/2} = \min\left(\lambda_1(\mathbf{U}_j), \lambda_1(\widehat{\mathbf{U}}_{j+1/2})\right),\tag{6.1a}$$

$$S_{\mathrm{R},j+1/2} = \max\left(\lambda_3(\widehat{\mathbf{U}}_{j+1/2}), \lambda_3(\mathbf{U}_{j+1})\right),\tag{6.1b}$$

where $\widehat{\mathbf{U}}$ denotes the Roe average of conserved variables. For the Euler equations, the eigenvalues are defined as $\lambda_1 = u - a$ and $\lambda_3 = u + a$, where u and a are the velocity and speed of sound, respectively. We note that the choice of wave velocity estimates is not a trivial matter and refer to Davis [4], Einfeldt [5] and Toro et al. [39] for detailed discussions about a number of different estimates and their properties. Herein, we choose (6.1) based on our own experience, where this choice yielded very good results, especially when it came to calculating entropy satisfying solutions. A more rigorous comparison between different wave velocity estimates in the LTS framework may be very fruitful, but at the moment it remains outside the scope of this paper.

In all the numerical experiments below, the input discretization parameters were the Courant number C and Δx. Then, the time step Δt was evaluated at each time step according to:

$$\Delta t = \frac{C\Delta x}{\max\limits_{p,x}|\lambda_p(x,t)|},\tag{6.2}$$

where λ_p are the eigenvalues of the Jacobian matrix $\mathbf{A}$ in (2.2).

6.1. Sod shock tube

As a first test case we consider the classic Sod shock tube problem [33], with initial data $\mathbf{V}(x,0) = (\rho, u, p)^\mathrm{T}$:

$$\mathbf{V}(x,0) = \begin{cases} (1,0,1)^\mathrm{T} & \text{if } x < 0, \\ (0.125,0,0.1)^\mathrm{T} & \text{if } x > 0, \end{cases}\tag{6.3}$$

where the solution is evaluated at $t = 0.4$ on a grid with 100 cells. Figure 3 shows the results obtained with HLL(C) and LTS-HLL(C) schemes with $C = 1$ and $C = 3$. We observe that the LTS-HLL scheme (Figure 3a) increases the accuracy of the shock and the left going part of the rarefaction wave, while increasing the diffusion of the contact discontinuity. This is in agreement with the results from section 5.2 and it is due to the fact that the standard HLL scheme assumes a two wave structure of the solution and neglects the contact discontinuity, leading to excessive diffusion. Since the LTS-HLL scheme maintains the two wave assumption, it can be seen that the increase in the time step leads to further smearing of the contact discontinuity. The LTS-HLLC scheme (Figure 3b) also improves the accuracy of the shock and the rarefaction wave. In addition, the LTS-HLLC

scheme also improves the accuracy of the contact discontinuity, because the HLLC scheme resolves the wave missing in the HLL scheme. The velocity profiles show that the LTS-HLLC scheme produces more spurious oscillations than the LTS-HLL scheme.

(A) Standard HLL and LTS-HLL scheme
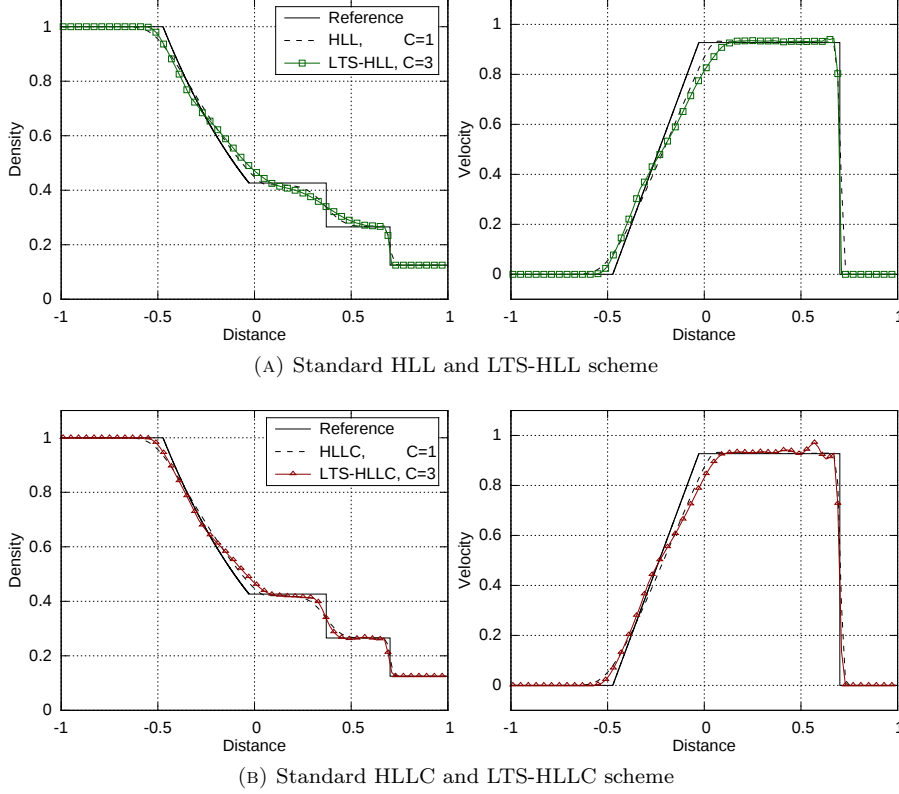

(B) Standard HLLC and LTS-HLLC scheme

FIGURE 3. Comparison between the standard HLL(C) and the LTS-HLL(C) schemes for the problem (6.3)

Next, we compare the performance of the LTS methods to each other. We consider the same test case and also include the results obtained with the LTS-Roe scheme [19]. Figure 4 shows that the LTS-Roe scheme produces spurious oscillations in both density and internal energy. Further, we observe that the LTS-Roe scheme violates the entropy condition, while both LTS-HLL and LTS-HLLC schemes produce entropy satisfying solutions. We note that for this test case, the standard Roe scheme does not lead to an entropy violation because there is no sonic point across the rarefaction wave. Lindqvist et al. [19] showed how the LTS-Roe scheme can lead to an entropy violation even if there is no sonic point across the rarefaction wave. Such an LTS-related entropy violation cannot be fixed with standard entropy fixes developed for the Roe scheme, but it can be fixed by splitting the rarefaction wave into several expansion shocks [13, 15, 31, 23, 41] or by varying the time step [18, 19]. Prebeg [29] showed that the LTS-HLL scheme with the wave velocity estimates (6.1) always produces entropy satisfying solutions.

Last, we investigate the computational times for the LTS-HLL(C) schemes at different Courant numbers and different grids, see Figure 5. We observe that for any grid, the CPU time decreases as we increase the Courant number. However, by looking at the CPU time required to reach the same error we observe that the HLL scheme tends to be more efficient than the LTS-HLL scheme, and that the LTS-HLLC scheme tends to be more efficient than the HLLC scheme.
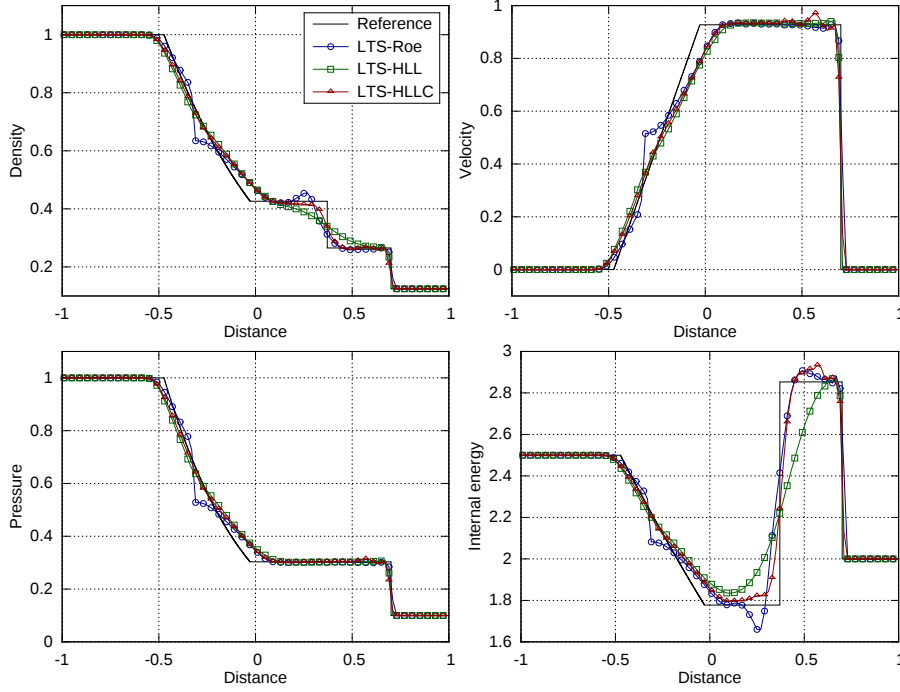
FIGURE 4. Comparison between different LTS schemes at $C = 3$ for problem (6.3)
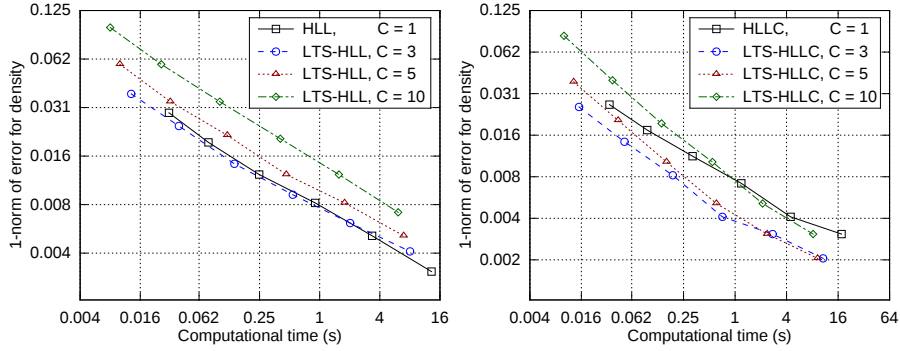
FIGURE 5. Computational time vs. error estimate $\mathcal{E}$ for density with the LTS-HLL(C) schemes for the problem (6.3) with 100, 200, 400, 800, 1600 and 3200 cells

Remark 1. The CPU times are obtained with the MATLAB tic-toc function and averaged over a number of simulations. The computational times in Figure 5 correspond to implementation in the framework (2.5) with the numerical flux functions evaluated with (3.15) for the LTS-HLL and (4.7) for the LTS-HLLC scheme. We note that for the LTS-HLL scheme the similar computational efficiency trends are observed for implementations in the numerical viscosity framework (2.13) with (3.21), and the flux-difference splitting framework (2.14) with (3.26). Similar computational efficiency trends were reported by Lindqvist and Lund [18] and Prebeg et al. [30].

6.2. **Woodward-Colella blast-wave problem**

We consider the Woodward-Colella blast-wave problem [40]. The initial data is given by uniform density $\rho(x,0) = 1$, uniform velocity $u(x,0) = 0$, and two discontinuities in the pressure:

$$p(x,0) = \begin{cases} 1000 & \text{if} & 0 < x < 0.1, \\ 0.01 & \text{if} & 0.1 < x < 0.9, \\ 100 & \text{if} & 0.9 < x < 1. \end{cases} \tag{6.4}$$

The solution is evaluated at $t = 0.038$ on a grid with 500 cells. The solution consists of contact discontinuities at $x = 0.6$, $x = 0.76$ and $x = 0.8$ and shock waves at $x = 0.65$ and $x = 0.87$, see [17]. The boundary walls at $x = 0$ and $x = 1$ are modeled as reflective boundary condition. The reference solution was obtained by the Roe scheme with the superbee wave limiter on the grid with 16000 cells.

Figure 6 shows the results obtained with the standard HLLC scheme at $C = 1$ and different LTS methods at $C = 5$. We observe that both LTS-Roe and LTS-HLLC schemes are more accurate than the standard HLLC scheme. Next, we observe that all schemes correctly capture the positions of both shocks and contact discontinuities. As expected, all schemes resolve the shocks much more accurately than the contact discontinuities, especially the LTS-HLL scheme which introduces very strong diffusion at the contact discontinuities.
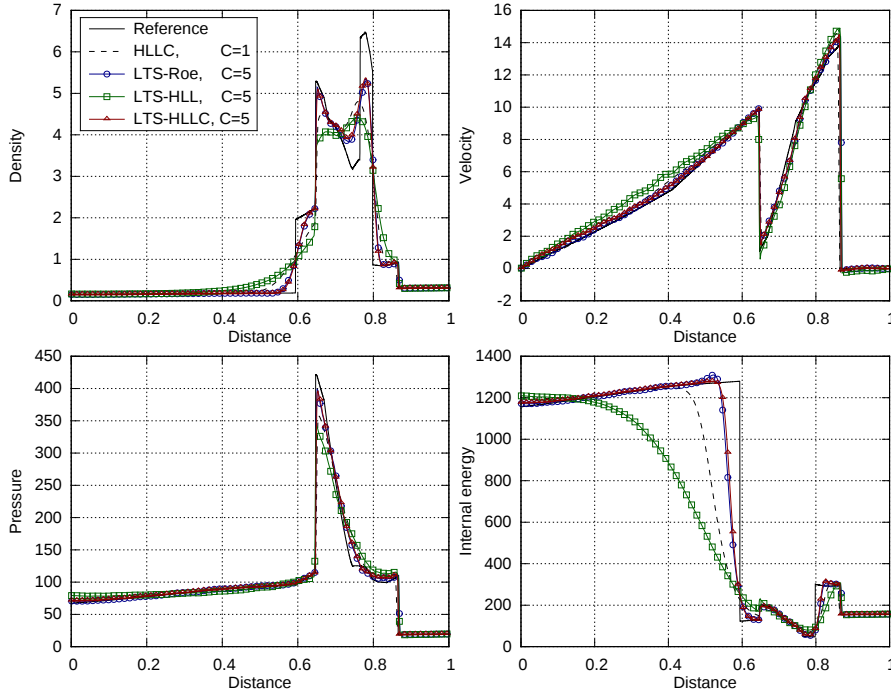

FIGURE 6. Comparison between the standard HLLC and different LTS methods for problem (6.4)

Last, we investigate the computational time for the LTS-HLL(C) schemes at different Courant numbers and different grids, see Figure 7. We observe that for any grid, the CPU time decreases as we increase the Courant number. For the LTS-HLL scheme, the optimal choice of the Courant number depends on the grid size. The LTS-HLLC scheme is always more efficient than the HLLC scheme. The observations made in Remark 1 also apply for Figure 7.
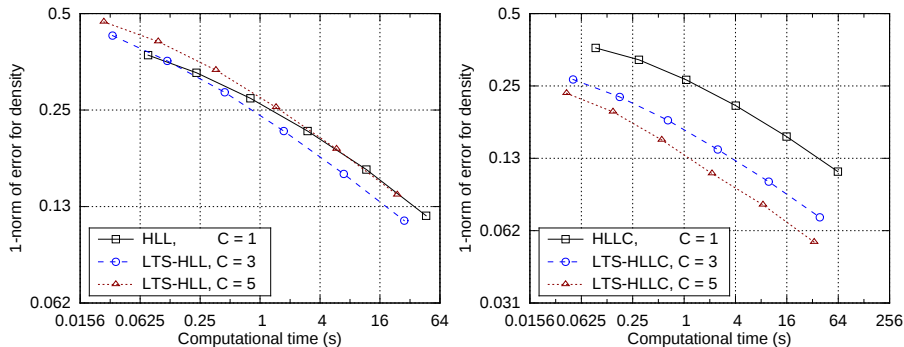
FIGURE 7. Computational time vs. error estimate $\mathcal{E}$ for density with the LTS-HLL(C) schemes for the problem (6.4) with 100, 200, 400, 800, 1600 and 3200 cells

7. CONCLUSIONS

Following LeVeque [15], previous works on Large Time Step (LTS) explicit methods have focused on the LTS-Roe and LTS-Godunov Riemann solvers. Aiming to achieve a more general platform for LTS methods, we have here formulated LTS versions of the HLL and HLLC approximate Riemann solvers. In particular, we have determined the explicit expressions for the flux-difference splitting coefficients and the numerical viscosity coefficients of the LTS-HLL scheme through our Propositions 2 and 3.

Through a modified equation analysis, we are able to precisely quantify the numerical diffusion associated with LTS approximate Riemann solvers. So far, the lack of a controlled mechanism for introducing stabilizing numerical diffusion has been a drawback for LTS methods [41]. In this respect, our Proposition 6 may be of interest, as it allows for interpreting S_L and S_R as parameters for smoothly controlling the numerical diffusion within the TVD region.

We applied the LTS-HLL(C) schemes to one-dimensional test cases for the Euler equations. At moderate Courant numbers the LTS-HLL scheme leads to increased accuracy of shocks and rarefaction waves compared to the standard HLL scheme. The stabilizing excessive diffusion on the contact wave is evident. For moderate Courant numbers, the LTS-HLLC scheme leads to an increased accuracy of shocks, rarefaction waves and contact discontinuities compared to the standard HLLC scheme. It also shows potential for increased robustness compared to the previously investigated LTS-Roe scheme [15, 19, 31]. We observe that for the Einfeldt's [5] choice of velocity estimates, both the LTS-HLL and LTS-HLLC schemes calculate entropy satisfying solutions. This is in agreement with a recent result by Prebeg [29] where the modified equation analysis was used to show that the LTS-HLL scheme with Einfeldt's choice of velocity estimates yields entropy satisfying solutions. This is a notable improvement compared to the existing LTS-Roe scheme for which entropy violations are observed for even more cases than with the standard Roe scheme [19, 31, 23]. For moderate Courant numbers, the LTS-HLLC scheme tends to be more efficient than the standard HLLC scheme in achieving a giving accuracy. For larger Courant numbers, both the LTS-HLL and LTS-HLLC schemes produced spurious oscillations and the accuracy decreased.

Further investigations are needed for robust higher order extensions of LTS methods, which were already considered by LeVeque [16] and Harten [8]. Moreover, conditions for preservation of positivity should be explored for LTS methods.

REFERENCES

[1] P. Batten, N. Clarke, C. Lambert, and D. M. Causon. "On the Choice of Wavespeeds for the HLLC Riemann Solver". *SIAM J. Sci. Comput.* 18 (6) (1997), pp. 1553–1570.

[2] F. Daude and P. Galon. "On the Computation of the Baer–Nunziato Model Using ALE Formulation with HLL- and HLLC-Type Solvers Towards Fluid–Structure Interactions". *J. Comput. Phys.* 304 (2016), pp. 189–230.

[3] F. Daude, P. Galon, Z. Gao, and E. Blaud. "Numerical Experiments Using a HLLC-Type Scheme With ALE Formulation for Compressible Two-Phase Flows Five-Equation Models With Phase Transition". *Comput. Fluids* 94 (2014), pp. 112–138.

[4] S.F. Davis. "Simplified Second-Order Godunov-Type Methods". *SIAM J. Sci. Stat. Comput.* 9 (3) (1988), pp. 445–473.

[5] B. Einfeldt. "On Godunov-Type Methods for Gas Dynamics". *SIAM J. Numer. Anal.* 25 (2) (1988), pp. 294–318.

[6] B. Einfeldt, C.-D. Munz, P.L. Roe, and B. Sjögreen. "On Godunov-Type Methods near Low Densities". *J. Comput. Phys.* 92 (2) (1991), pp. 273–295.

[7] A. Harten. "High Resolution Schemes for Hyperbolic Conservation Laws". *J. Comput. Phys.* 49 (3) (1983), pp. 357–393.

[8] A. Harten. "On a Large Time–Step High Resolution Scheme". *Math. Comp.* 46 (174) (1986), pp. 379–399.

[9] A. Harten, P. D. Lax, and B. van Leer. "On Upstream Differencing and Godunov-Type Schemes for Hyperbolic Conservation Laws". *SIAM Rev.* 25 (1) (1983), pp. 35–61.

[10] A. Jameson and P. D. Lax. "Conditions for the Construction of Multi-Point Total Variation Diminishing Difference Schemes". *Appl. Numer. Math.* 2 (3–5) (1986), pp. 335–345.

[11] A. Jameson and P. D. Lax. "Corrigendum: Conditions for the Construction of Multi-Point Total Variation Diminishing Difference Schemes". *Appl. Numer. Math.* 3 (3) (1987), p. 289.

[12] P. Janhunen. "A Positive Conservative Method for Magnetohydrodynamics Based on HLL and Roe Methods". *J. Comput. Phys.* 160 (2) (2000), pp. 649–661.

[13] R. J. LeVeque. "Large Time Step Shock-Capturing Techniques for Scalar Conservation Laws". *SIAM J. Numer. Anal.* 19 (6) (1982), pp. 1091–1109.

[14] R. J. LeVeque. "Convergence of a Large Time Step Generalization of Godunov's Method for Conservation Laws". *Comm. Pure Appl. Math.* 37 (4) (1984), pp. 463–477.

[15] R. J. LeVeque. "A Large Time Step Generalization of Godunov's Method for Systems of Conservation Laws". *SIAM J. Numer. Anal.* 22 (6) (1985), pp. 1051–1073.

[16] R. J. LeVeque. "High Resolution Finite Volume Methods on Arbitrary Grids via Wave Propagation". *J. Comput. Phys.* 78 (1) (1988), pp. 36–63.

[17] R.J. LeVeque. *Finite Volume Methods for Hyperbolic Problems*. Cambridge Texts in Applied Mathematics (Book 31). Cambridge University Press, 2002.

[18] S. Lindqvist and H. Lund. "A Large Time Step Roe Scheme Applied to Two-Phase Flow". In: *VII European Congress on Computational Methods in Applied Sciences and Engineering*. Ed. by M. Papadrakakis, V. Papadopoulos, G. Stefanou, and V. Plevris. Crete Island, Greece, 2016.

[19] S. Lindqvist, P. Aursand, T. Flåtten, and A. A. Solberg. "Large Time Step TVD Schemes for Hyperbolic Conservation Laws". *SIAM J. Numer. Anal.* 54 (5) (2016), pp. 2775–2798.

[20] H. Lochon, F. Daude, P. Galon, and J.-M Hérard. "HLLC-Type Riemann Solver with Approximated Two-Phase Contact for the Computation of the Baer–Nunziato Two-Fluid Model". *J. Comput. Phys.* 326 (2016), pp. 733–762.

[21] N. N. Makwana and A. Chatterjee. "Fast Solution of Time Domain Maxwell's Equations Using Large Time Steps". In: *2015 IEEE International Conference on Computational Electromagnetics (ICCEM 2015)*. Hong Kong, China: Institute of Electrical and Electronics Engineers (IEEE), 2015, pp. 330–332.

[22] T. Miyoshi and K. Kusano. "A Multi-State HLL Approximate Riemann Solver for Ideal Magnetohydrodynamics". *J. Comput. Phys.* 208 (1) (2005), pp. 315–344.

[23] M. Morales-Hernández, P. García-Navarro, and J. Murillo. "A Large Time Step 1D Upwind Explicit Scheme (CFL>1): Application to Shallow Water Equations". *J. Comput. Phys.* 231 (19) (2012), pp. 6532–6557.

[24] M. Morales-Hernández, M. Hubbard, and P. García-Navarro. "A 2D Extension of a Large Time Step Explicit Scheme (CFL>1) for Unsteady Problems with Wet/Dry Boundaries". *J. Comput. Phys.* 263 (2014), pp. 303–327.

[25] M. Morales-Hernández, J. Murillo, P. García-Navarro, and J. Burguete. "A Large Time Step Upwind Scheme for the Shallow Water Equations With Source Terms". In: *Numerical Methods for Hyperbolic Equations*. Ed. by Elena Vázquez Cendón, Arthuro Hidalgo, P. García-Navarro, and Luis Cea. CRC Press, 2012, pp. 141–148.

[26] M. Morales-Hernández, A. Lacasta, J. Murillo, and P. García-Navarro. "A Large Time Step Explicit Scheme (CFL>1) on Unstructured Grids for 2D Conservation Laws: Application to the Homogeneous Shallow Water Equations". *Appl. Math. Model.* 47 (2017), pp. 294–317.

[27] J. Murillo, P. García-Navarro, P. Brufau, and J. Burguete. "Extension of an Explicit Finite Volume Method to Large Time Steps (CFL>1): Application to Shallow Water Flows". *Int. J. Numer. Meth. Fluids* 50 (1) (2006), pp. 63–102.

[28] M. Pelanti and K.-M. Shyue. "A Mixture-Energy-Consistent Six-Equation Two-Phase Numerical Model for Fluids with Interfaces, Cavitation and Evaporation Waves". *J. Comput. Phys.* 259 (2014), pp. 331–357.

[29] M. Prebeg. "Numerical Viscosity in Large Time Step HLL-type Schemes". In: *Proceedings of the Sixteenth International Conference on Hyperbolic Problems, HYP2016*. Ed. by C. Klingenberg and M. Westdickenberg. Accepted for publication. Aachen, Germany, 2016.

[30] M. Prebeg, T. Flåtten, and B. Müller. "Large Time Step Roe Scheme for a Common 1D Two-Fluid Model". *Appl. Math. Model.* 44 (2017), pp. 124–142.

[31] Z. Qian and C.-H. Lee. "A Class of Large Time Step Godunov Schemes for Hyperbolic Conservation Laws and Applications". *J. Comput. Phys.* 230 (19) (2011), pp. 7418–7440.

[32] P. Roe. "Approximate Riemann Solvers, Parameter Vectors, and Difference Schemes". *J. Comput. Phys.* 43 (2) (1981), pp. 357–372.

[33] G. A. Sod. "A Survey of Several Finite Difference Methods for Systems of Nonlinear Hyperbolic Conservation Laws". *J. Comput. Phys.* 27 (1) (1978), pp. 1–31.

[34] E. Tadmor. "Numerical Viscosity and the Entropy Condition for Conservative Difference Schemes". *Math. Comp* 43 (168) (1984), pp. 369–381.

[35] K. Tang, A. Beccantini, and C. Corre. "Combining Discrete Equations Method and Upwind Downwind-Controlled Splitting for Non-Reacting and Reacting Two-Fluid Computations: One Dimensional Case". *Comput. Fluids* 93 (2014), pp. 74–90.

[36] B. Tian, E. F. Toro, and C. E. Castro. "A Path-Conservative Method for a Five-Equation Model of Two-Phase Flow with an HLLC-Type Riemann Solver". *Comput. Fluids* 46 (1) (2011), pp. 122–132.

[37] S. A. Tokareva and E. F. Toro. "HLLC-Type Riemann Solver for Baer–Nunziato Equations of Compressible Two-Phase Flow". *J. Comput. Phys.* 229 (10) (2010), pp. 3573–3604.

[38] E. F. Toro. *Riemann Solvers and Numerical Methods for Fluid Dynamics*. 3rd ed. Springer-Verlag Berlin Heidelberg, 2009.

[39] E. F. Toro, M. Spruce, and W. Speares. "Restoration of the Contact Surface in the HLL-Riemann Solver". *Shock Waves* 4 (1) (1994), pp. 25–34.

[40] P. Woodward and P. Colella. "The Numerical Simulation of Two-Dimensional Fluid Flow with Strong Shocks". *J. Comput. Phys.* 54 (1) (1984), pp. 115–173.

[41] R. Xu, D. Zhong, B. Wu, X. Fu, and R. Miao. "A Large Time Step Godunov Scheme for Free-Surface Shallow Water Equations". *Chinese Sci. Bull.* 59 (21) (2014), pp. 2534–2540.

[42] G.-S. Yeom and K.-S. Chang. "Two-Dimensional Two-Fluid Two-Phase Flow Simulation Using an Approximate Jacobian Matrix for HLL Scheme". *Numer. Heat Tr. B-Fund.* 56 (5) (2010), pp. 372–392.